An Electron-Attractor Model: FM Nanoclusters Responsible for Magnetoresistant Behavior in Ca-Rich $La_{1-x}Ca_xMnO_3$

Raquel Cortés-Gil,[†,‡] José M. Alonso,[‡,§] M. Luisa Ruiz-González,[†] María Vallet-Regí,[‡,||] Antonio Hernando,[‡,⊥] and José M. González-Calbet*[,†,‡]

Departamento de Química Inorgánica, Facultad de Químicas, Universidad Complutense, 28040-Madrid, Spain, Instituto de Magnetismo Aplicado, UCM-CSIC-ADIF, Las Rozas, P.O. Box 155, 28230-Madrid, Spain, Instituto de Ciencia de Materiales, CSIC, Sor Juana Inés de la Cruz s/n, 28049-Madrid, Spain, Departamento de Química Inorgánica y Bioinorgánica, Facultad de Farmacia, Universidad Complutense, 28040-Madrid, Spain, and Departamento de Física de Materiales, Facultad de Físicas, Universidad Complutense, 28040-Madrid, Spain

Received January 24, 2008. Revised Manuscript Received March 3, 2008

On the basis of magnetization and resistivity measurements in the $La_{1-x}Ca_xMnO_3$ system, a model is proposed for explaining the complex magnetic and magnetoresistant behavior along the $0.80 < x < 1$ composition range. This model assumes localization of Mn^{3+} cations around La^{3+} substitutional atoms resulting in ferromagnetic nanoclusters, of about 0.9 nm size, due to double exchange interactions with Mn^{4+} surrounding being responsible for magnetoresistant behavior. The proposed model allows one to explain the magnetic behavior of both hole and electron doping regions in the $La_{1-x}Ca_xMnO_3$ system.

Introduction

The $Ln_{1-x}A_xMnO_3$ (Ln = lanthanide, A = earth alcaline) system tends to exhibit phase separation, usually antiferromagnetic (AFM) and ferromagnetic (FM), which has been theoretically predicted[1–4] but also experimentally probed by different techniques.[2,3] The study of this system through analytic models based on Hamiltonian resolution is quite complicated due to the existence of phase segregation. However, this Hamiltonian gives rise to satisfactory results to explain experimental facts such as the existence of AFM phases for $x = 0$ (A-type) and $x = 1$ (G-type),[5] the appearance of a FM phase for intermediate values,[6,7] the existence of orbital, charge, and spin ordering[8] for $x = 0.5$, and, even more, the tendency of these systems to exhibit nanometric phase separation, which seems to be crucial to explain the colossal magnetoresistance (CMR). Ferromagnetic clusters of nanometric size, imbibed in an AFM matrix, have been observed in the $Ln_{1-x}A_xMnO_3$ systems for low hole[9–12] or electron[13–16] densities, that is, for x extreme values where the doping concentration is small. Ling and Granado[15,16] have shown the formation of FM nanometric clusters in the calcium-rich region, whose number increases as x decreases in the $0.93 \leq x \leq 1$ range, keeping its size constant, with a diameter around 1 nm, imbibed in a G-type AFM matrix characteristic of $CaMnO_3$. However, despite the enormous amount of magnetic information, few studies about their electric behavior have been reported in this region.[13,17,18]

Electrical measurements could supply important information on the origin and nature of these nanometric clusters and so about the phase separation. To explain these features, Meskine and Satpathy[19] have recently proposed a model of self-trapped magnetic polarons, which comprises a central Mn atom and the six adjacent showing a magnetic moment, calculated from the density-functional theory, of 6.68 μ_B.

The origin of these clusters is still an open question. Quenched disorder has been considered as a plausible cause of the existence

* To whom correspondence should be addressed. E-mail: jgcalbet@quim.ucm.es. Fax: 34 91 394 43 52.
† Departamento de Química Inorgánica, Universidad Complutense.
‡ UCM-CSIC-ADIF.
§ CSIC.
|| Departamento de Química Inorgánica y Bioinorgánica, Universidad Complutense.
⊥ Departamento de Física de Materiales, Universidad Complutense.

(1) Millis, A. J. Theory of CMR Manganites. In *Colossal Magnetoresistance Oxides*, Advances in Condensed Matter Science; Tokura, Y., Ed.; Gordon & Breach Science Publishers: Langhorne, PA, 2000; Vol 2.
(2) Dagotto, E.; Hotta, T.; Moreo, A. *Phys. Rep.* **2001**, *344*, 1–153.
(3) Dagotto, E. *Solid State Science, "Nanoscale Phase Separation and Colossal Magnetoresistance"*; Springer: New York, 2003.
(4) Gorkov, L. P.; Kresin, L. P. *Phys. Rep.* **2004**, *400*, 149–208.
(5) Wollan, E. O.; Koehler, W. C. *Phys. Rev.* **1955**, *100*, 545–563.
(6) Cheong, C. W.; Hwang, H. Y. Ferromagnetism vs Charge/Orbital Ordering in Mixed-Valent Manganites. In *Colossal Magnetoresistance Oxides*, Advances in Condensed Matter Science; Tokura, Y., Ed.; Gordon & Breach Science Publishers: Langhorne, PA, 2000; Vol. 2.
(7) Schiffer, P.; Ramirez, A. P.; Bao, W.; Cheong, S.-W. *Phys. Rev. Lett.* **1995**, *75*, 3348–3351.
(8) Chen, C. H.; Cheong, S.-W. *Phys. Rev. Lett.* **1996**, *76*, 4042–4045.
(9) Hennion, M.; Moussa, F.; Biotteau, G.; Rodríguez-Carvajal, J.; Pinsard, L.; Revcolevschi, A. *Phys. Rev. Lett.* **1998**, *81*, 1957–1960.
(10) Allodi, G.; De Renzi, R.; Guidi, G. *Phys. Rev. B* **1998**, *57*, 1024–1034.
(11) Herrero, E.; Alonso, J.; Martínez, J. L.; Vallet-Regí, M.; Gonzalez-Calbet, J. M. *Chem. Mater.* **2000**, *12*, 1060–1066.
(12) Alonso, J.; Herrero, E.; González-Calbet, J. M.; Vallet-Regí, M.; Martínez, J. L.; Rojo, J. M.; Hernando, A. *Phys. Rev. B* **2000**, *62*, 11328–11331.
(13) Neumeier, J. J.; Cohn, J. L. *Phys. Rev. B* **2000**, *61*, 14319–14322.
(14) Respaud, M.; Broto, J. M.; Rakoto, H.; Vanacken, J.; Wagner, P.; Martin, C.; Maignan, A.; Raveau, B. *Phys. Rev. B* **2001**, *63*, 1444261–6.
(15) Ling, C. D.; Granado, E.; Neumeier, J. J.; Lynn, J. W.; Argyriou, D. N. *Phys. Rev. B* **2003**, *68*, 1344391–8.
(16) Granado, E.; Ling, C. D.; Neumeier, J. J.; Lynn, J. W.; Argyriou, D. N. *Phys. Rev. B* **2003**, *68*, 1344401–6.
(17) Martin, C.; Maignan, A.; Hervieu, M.; Raveau, B. *Phys. Rev. B* **1999**, *60*, 12191–12199.
(18) Chiorescu, C.; Neumeier, J. J.; Cohn, J. L. *Phys. Rev. B* **2006**, *73*, 10144061–6.
(19) Meskine, H.; Satpathy, S. *J. Phys.: Condens. Matter* **2005**, *17*, 1889–1906.

10.1021/cm800240v CCC: $40.75
Published on Web 04/18/2008

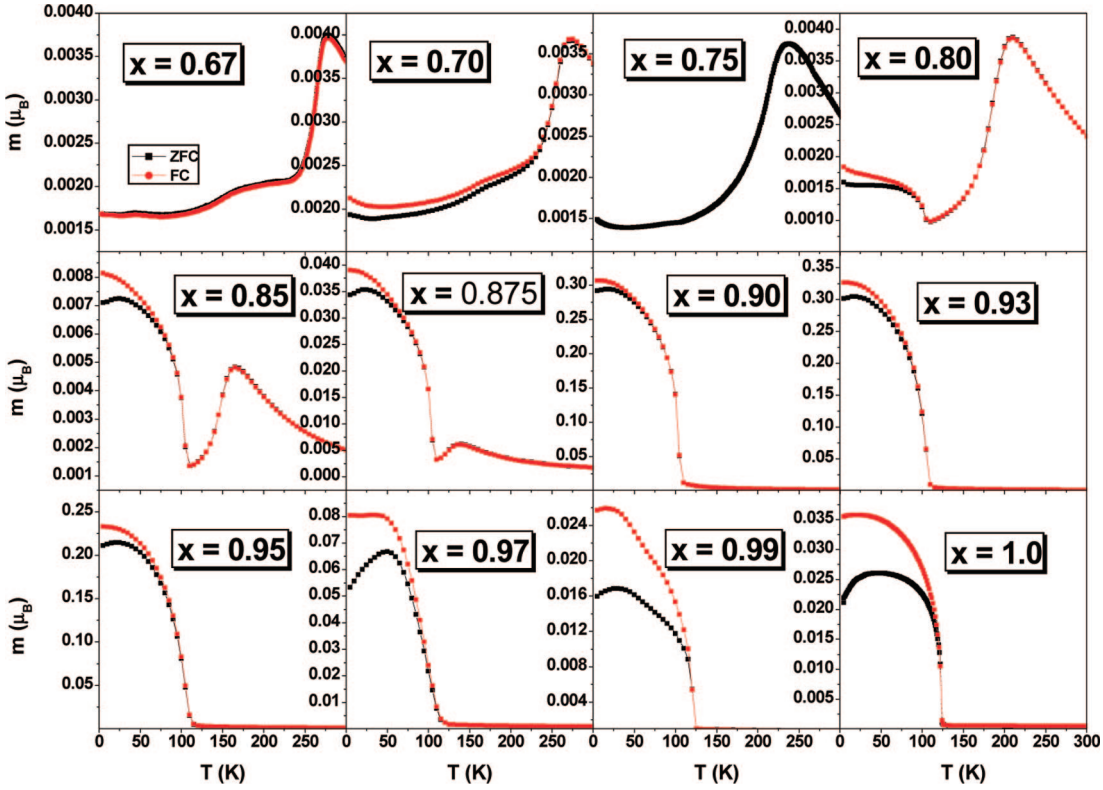

Figure 1. Magnetization evolution, in ZFC and FC conditions, as a function of the temperature at applied magnetic field of 1000 Oe, in the $La_{1-x}Ca_xMnO_3$ system ($0.67 \leq x \leq 1$).

of this phase segregation.[20,21] Such disorder is, inevitably, introduced when substituting the lanthanide cation by an earth alkaline one, which has never been taken into account in the theoretical models explaining the manganites' behavior. In this sense, several experiments[11,12,22–25] suggest that the divalent substituting ions, in addition to providing holes to the system, act as effective attractors for these holes. Actually, for a constant Mn^{4+} concentration, it is possible to drastically modify the compound properties by changing the alkaline earth concentration, which suggests that such cation can play an important role in the properties of this and similar systems.[22,23] From experimental results and taking into account the magnetic and magnetotransport properties, we propose a model in which localization of Mn^{3+} around La^{3+} substitutional atoms is assumed in the low electron concentration region.

Experimental Details

Powdered $La_{1-x}Ca_xMnO_3$ ($0.67 \leq x \leq 1$) materials were prepared by ceramic method at 1400 °C for 110 h. The cationic composition was determined by X-ray energy dispersive spectroscopy (XEDS) performed on an Oxford Isis spectrometer coupled on a JEOL 2000FX transmission electron microscope. Oxygen content, and therefore Mn^{4+}/Mn^{3+} ratio, was determined by thermogravimetric analysis (TGA) in a CAHN-D200 electrobalance. The cationic and anionic composition was found to be in agreement with the nominal one.

Structural characterization was performed by X-ray diffraction (XRD) with a Philips X'Pert diffractometer equipped with a Cu Kα radiation source and by selected area electron diffraction (SAED) with a JEOL 2000FX electron microscope. All samples exhibited perovskite-type structure with orthorhombic symmetry and *Pnma* space group.

The magnetic properties were determined with a Quantum Desing SQUID magnetometer in the temperature range from 5 to 300 K at applied fields of up to 5 T. The resistance measurements were carried out by the four contacts method by means of PPMS (Quantum Desing) in the 5–400 K range and fields of up to 9 T.

Results and Discussion

The complex magnetic behavior of the $La_{1-x}Ca_xMnO_3$ system in the Ca-rich region is well-known, being a characteristic example of phase segregation in manganites.[15,16] This fact is reflected in Figure 1, which shows the magnetization evolution, as a function of the temperature, in zero magnetic field (ZFC) and magnetic field cooling (FC) conditions, along the $0.67 \leq x \leq 1$ composition range. As it can be observed, different magnetic phases exist as a function of x. The spontaneous magnetization evolution with Ca concentration is depicted in Figure 2. These values are obtained from magnetization measurements versus applied magnetic field at 5 K (not shown here). As is usually done,[16] the curve is discomposed into a FM signal, which saturates at spontaneous magnetization (see Figure 2 and Table 1) and a linear component corresponding to an AFM contribution. In this way, the spontaneous magnetization values are obtained by subtraction of AFM contribution at 5 K and $H = 0$.

(20) Tokura, Y. *Rep. Prog. Phys.* **2006**, *69*, 797–851.
(21) Dagotto, E. *Science* **2005**, *309*, 257–262.
(22) Alonso, J. M.; Arroyo, A.; González-Calbet, J. M.; Vallet-Regí, M.; Martínez, J. L.; Rojo, J. M.; Hernando, A. *Phys. Rev. B* **2001**, *64*, 1724101–4.
(23) Alonso, J. M.; Arroyo, A.; González-Calbet, J. M.; Hernando, A.; Rojo, J. M.; Vallet-Regí, M. *Chem. Mater.* **2003**, *15*, 2864–2866.
(24) Shibata, T.; Bunker, B. A.; Mitchell, J. F. *Phys. Rev. B* **2003**, *68*, 0241031–10.
(25) Battabyal, M.; Dey, T. K. *Physica B* **2005**, *367*, 40–47.

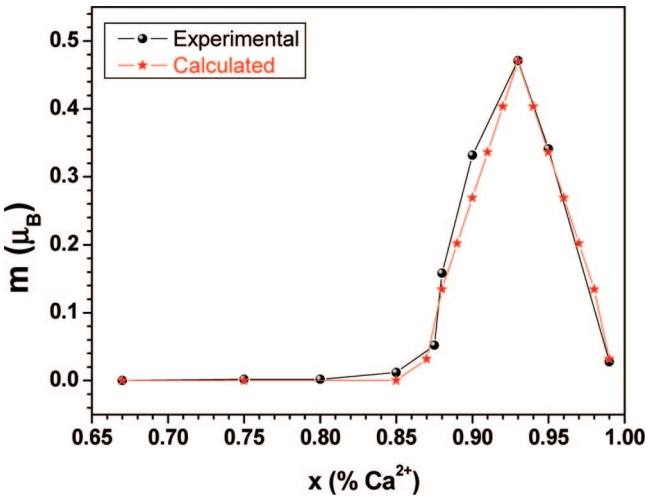

Figure 2. Calculated and experimental spontaneous magnetization evolution with Ca concentration in $La_{1-x}Ca_xMnO_3$ ($0.67 \leq x \leq 1$).

Table 1. Calculated and Experimental m_s Values for Each x Value in the $La_{1-x}Ca_xMnO_3$ System

x	m_s (μ_B) calculated	m_s (μ_B) experimental
0.99	0.032	0.027
0.97	0.202	0.205
0.95	0.336	0.341
0.93	0.470	0.471
0.90	0.269	0.352
0.88	0.134	0.158
0.875	0.083	0.052
0.85	0.00	0.012
0.80	0.00	0.002
0.75	0.00	0.002

These results agree with previous works,[15,16] being a consequence of the alteration of the $CaMnO_3$ matrix when La doping is induced. Actually, $CaMnO_3$ exhibits a G-type AFM structure (T_N = 122 K), and the La introduction provides electrons (Mn^{3+}) giving rise to nanometric FM droplets inside AFM matrix.[15,16] As the La substitution increases, the droplets concentration also increases, although not their sizes, hitherto a maximum value for $x = 0.93$. For higher La content, the FM droplets as well as the G-type AFM matrix begin disappearing while a C-type AFM phase is promoted. This new ordering is almost complete for $x \leq 0.8$ and starts, again, its transformation toward a Wigner

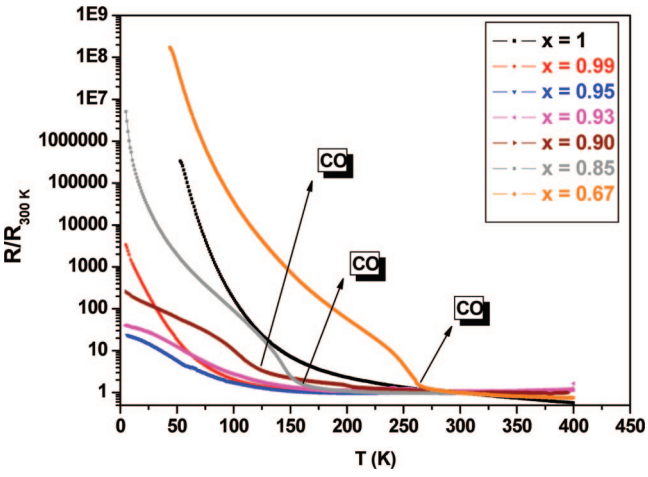

Figure 3. The electrical resistance as a function of the temperature in the $La_{1-x}Ca_xMnO_3$ system ($0.67 \leq x \leq 1$).

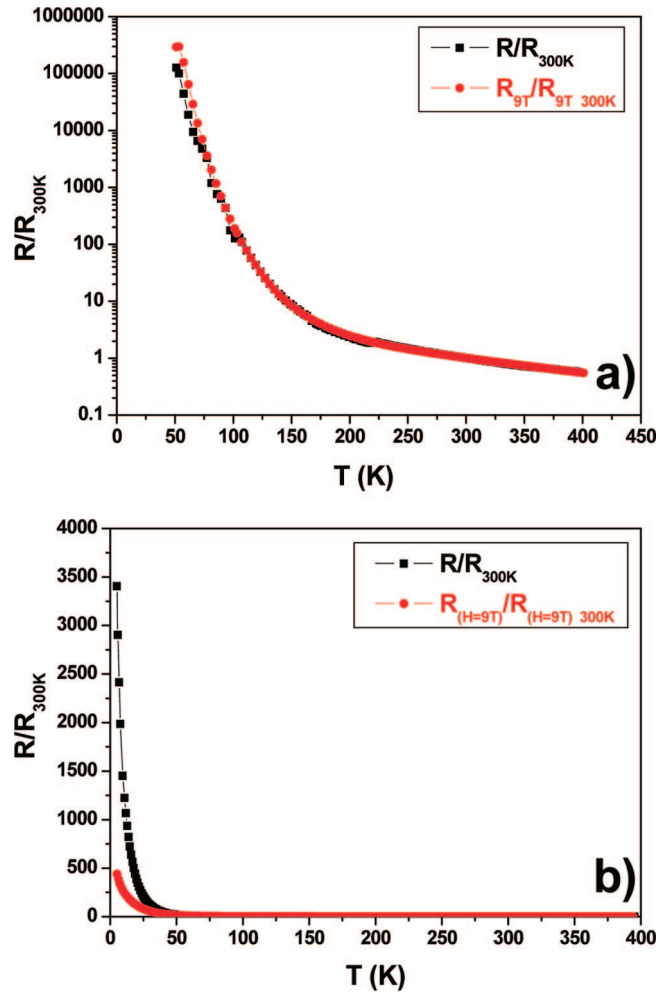

Figure 4. Electrical resistance measurements with and without applied magnetic field as a function of the temperature corresponding to (a) $CaMnO_3$ and (b) $La_{0.01}Ca_{0.99}MnO_3$.

Crystal (WC). According to these facts, it is clear that for $0.8 < x < 1$, the $La_{1-x}Ca_xMnO_3$ system can be described as an AFM matrix with imbibed FM clusters.

The variation of the electrical resistance as a function of the temperature is shown in Figure 3. As it is well-known, $CaMnO_3$ exhibits semiconductor behavior with high resistance values at low T (10^5 Ω at 60 K). However, the introduction of 1% La (1% electrons) produces a drastic decrease of the resistance, being 4 orders of magnitude less at 60 K (Figure 3). A continuous decreasing of the resistance is observed as the lanthanum concentration increases up to around 7% La, that is, $La_{0.07}Ca_{0.93}MnO_3$. For higher La content, the resistance increases again. It is worth recalling that for $La_{0.15}Ca_{0.85}MnO_3$ and $La_{0.33}Ca_{0.67}MnO_3$ the resistance suddenly increases at 165 and 270 K, respectively. This fact is related to a charge ordering (CO) state. $La_{0.10}Ca_{0.90}MnO_3$ also shows, although less markedly, an increase in the resistance value at 110 K, suggesting, again, the presence of a certain charge ordering fraction. The ensemble of this data indicates the enormous complexity of the system around $x \approx 0.90$ because of the coexistence of CO with two AFM structures (C and G) and FM droplets. Under these circumstances, it is mandatory to search the possible magnetoresistant behavior in this region.

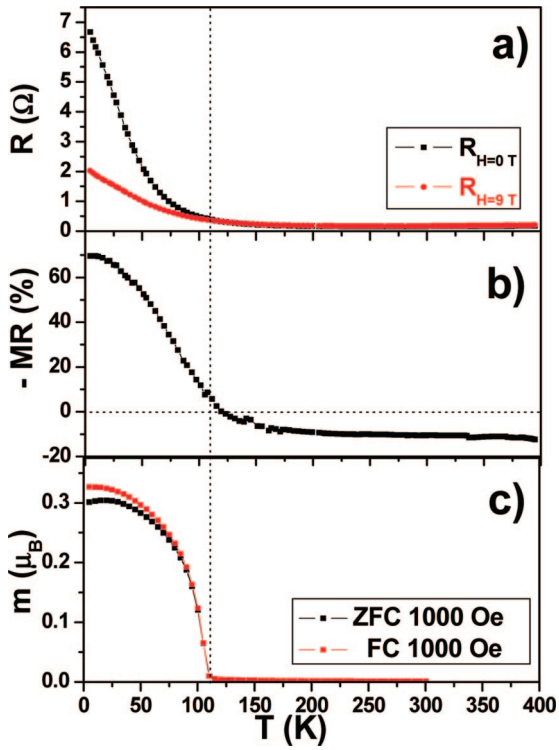

Figure 5. (a) Resistance measurements with and without applied magnetic field. (b) Magnetoresistance and (c) magnetization with and without applied magnetic field, as a function of the temperature corresponding to $La_{0.07}Ca_{0.93}MnO_3$.

Actually, Martin et al.[17] have proposed a phase diagram where CMR is only present in a very short compositional range $0.89 \leq x < 0.92$. However, because FM clusters appear in a broader $0.80 < x < 1$, it is worth studying the magnetotransport properties in this range. The resistance measurement performed in the absence or presence of the magnetic field in $CaMnO_3$ (Figure 4a) indicates the absence of magnetoresistance. However, the introduction of only 1% of La involves a different behavior with respect to the undoped sample. In the case of $La_{0.01}Ca_{0.99}MnO_3$, the application of a magnetic field produces a decrease in the resistance, indicating the presence of magnetoresistance with negative character (Figure 4b). This behavior is related to the presence of FM clusters.

The resistance and the magnetization (with and without applied magnetic field) and the magnetoresistance as a function of temperature are represented in Figure 5. For $T \leq 112$ K, coinciding with the FM clusters appearance, $La_{0.07}Ca_{0.93}MnO_3$ exhibits CMR with a maximum value of 70% at 5 K. The fact that both phenomena, FM and CMR, appear at the same temperature suggests the same origin, which is the double exchange mechanism. In this sense, it is worth recalling that CMR appears when isolated FM clusters are present, that is, in the $0.9 \leq x < 1$ compositional range. Moreover, up to T_c, the sign of the magnetoresistance changes, indicating that the double exchange mechanism has disappeared and a conventional mechanism takes place. Along this temperature range ($T > T_c$), the magnetic field induces the increase of the resistance, rendering a magnetoresistant positive character.

From these results, it is possible to estimate the size and magnetic contribution of the responsible entities for the magnetotransport properties by means of a model in the Ca-rich region similar to that previously proposed[22,23] in the La-rich one, considering that the La^{3+} doping in $CaMnO_3$ leads to $Mn^{4+} \rightarrow Mn^{3+}$ reduction (electron doping). In this sense, it can be assumed, as for high x values, that to keep the lattice electroneutrality, Mn^{3+} is located close to La^{3+}, while double exchange interactions Mn^{3+}–O–Mn^{4+} are produced around this cation, giving rise to FM clusters that do not perturb the G-type matrix ($CaMnO_3$). In this sense, a direct relation between the clusters magnetic moment and the saturation magnetization value (m_s) can be considered.

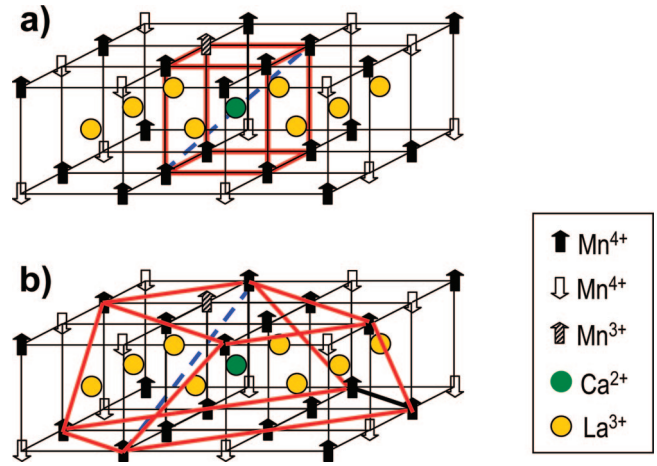

Figure 6. Schematic representation of FM clusters in the Ca-rich region in the $La_{1-x}Ca_xMnO_3$ system taking into account (a) 8 and (b) 16 Mn ions.

Actually, on the basis of the perovskite cell, it seems reasonable to assume that the cluster is built up from one La^{3+} cation surrounded by 7 Mn^{4+} and one Mn^{3+} (see Figure 6a). The Mn^{3+} introduced is FM coupled with Mn^{4+} neighbors via double exchange and is placed randomly in this cubic subcell in agreement with the Goodenough model.[26] Besides, we propose that the origin of the FM behavior is a consequence of Mn^{3+} localization around La^{3+} to keep the lattice electroneutrality.

Considering the Mn^{3+} and Mn^{4+} magnetic moments ($\mu_{Mn3+} = 4.90\ \mu_B$, $\mu_{Mn4+} = 3.87\ \mu_B$), the cluster magnetic moment would be:

$$\mu_{cluster} = \sqrt{7 / 8(3.87)^2 + 1 / 8(4.90)^2} = 4.01\ \mu_B \qquad (1)$$

However, it must be also considered that eight Mn^{4+} ions, with their magnetic moments parallel orientated (Figure 6a), are surrounding the cluster, and therefore, the total magnetic moment would be:

$$\mu_{total} = \mu_{cluster} + 8 / 8(3.87) = 7.88\ \mu_B \qquad (2)$$

The m_s value would be obtained multiplying the magnetic moment corresponding to one cluster by the number of clusters $(1 - x)$:

$$m_s = (1 - x)\ [\mu_{cluster} + 8 / 8(3.87)] \qquad (3)$$

Taking into account this expression, the m_s values obtained are slightly higher than the experimental ones. For instance, for $x = 0.93$, the calculated value is 0.55 μ_B and the

(26) Goodenough, J. B. *Phys. Rev.* **1995**, *100*, 564–573.

experimental one is 0.47 μ_B (Table 1). A more complex FM cluster can be considered by including 16 Mn ions (Figure 6b), leading to the next formula for the magnetic cluster:

$$\mu_{total} = \sqrt{7 / 8(3.87)^2 + 1 / 8(4.90)^2 + 8 / 8(3.87)^2} = 5.57\ \mu_B \quad (4)$$

Following with the above example, $x = 0.93$, multiplying by the La^{3+} concentration (0.07), the magnetic moment results to be $m_s = 0.36\ \mu_B$, which is slightly smaller than the experimental one. However, if the values corresponding to the two kinds of clusters are averaged, the $m_s = 0.47\ \mu_B$, which is identical to the experimental one. It is worth remembering that the total average magnetic moment is 6.72 μ_B, which is almost identical to the one obtained by H. Meskine and S. Satpathy,[19] following their model of self-trapped magnetic polarons.

A similar fit between experimental and calculated results is obtained for m_s in the $0.93 \leq x \leq 1$ range (Table 1), indicating that the FM clusters are, in fact, intermediate between the two ideal situations depicted in Figure 6a and b. The cluster size can be estimated from the maximum distance between Mn cations (marked in Figure 6) in one cluster taking into account the parameter of the perovskite cubic subcell $a_c \approx 0.37$ nm. For the smaller cluster (Figure 6a):

$$d_{max} = \sqrt{a_c^2 + a_c^2 + a_c^2} = 0.65\ \text{nm} \quad (5)$$

while for the bigger one (Figure 6b):

$$d_{max} = \sqrt{(3a_c)^2 + a_c^2} = 1.19\ \text{nm} \quad (6)$$

with 0.92 nm being the average size. This value is in agreement with the data obtained from neutron diffraction measurements:[16] ~1 nm.

It can then be observed that the model we propose, based on the Mn^{3+} localization around La^{3+}, leads to results in agreement with the experimental data in the $0.93 \leq x \leq 1$ range. The model qualitatively explains the origin of the FM droplets while, quantitatively, reproducing their size and the m_s value, for each sample. A different situation is observed for $x < 0.93$ because the probability of finding isolated La^{3+} decreases, as seen in Figure 2. At this point, it is worth remembering that the percolation threshold in the rich-lanthanum region is attained for $x = 0.125$.[11,12] In the Ca-rich region, assuming a homogeneous La^{3+} distribution, the percolation would occur at $x = 0.875$. This suggests that La^{3+} cations remain isolated up to a theoretical value of $x = 0.9375$, which is medium value in the $0.875 \leq x \leq 1$ range, and therefore the increasing of the La concentration does not lead to more isolated clusters, but gives rise to their percolation process in such a way that the number of cluster decreases. Diffraction neutron studies[15,16] show that for $x \approx 0.93$ the so-called G-type AFM phase starts changing to the C-type AFM and almost disappears for $x \approx 0.8$. These facts suggest that the clusters percolation does not increase the clusters size but leads to the formation of a new AFM structure, which would explain the decrease of the magnetization value for $x < 0.93$. As a consequence of the cluster percolation, it can be assumed the decreasing of the number of isolated clusters, as x decreases, in agreement with the following equation:

$$n_{cluster} = 2n_{max} - (1 - x), \quad n_{max} = 0.93 \quad (7)$$

and then the m_s values would be obtained by multiplying the calculated magnetic moment corresponding to one cluster by the number of clusters. The results, gathered in Table 1, show a good agreement with the experimental ones (Figure 2). It is also worth mentioning that, for $x < 0.93$, both experimental and calculated m_{es} progressively decrease, vanishing at $x = 0.80$. This calcium content corresponds to the maximum ratio of the C-type AFM phase observed by Ling et al.[15]

Once again, the substituting ions, that is, La^{3+}, in addition to providing electrons to the system, act as effective attractors for these electrons, explaining the origin of the FM contribution in the $0.85 \leq x < 1$ range. Moreover, this contribution can be quantified because isolated FM clusters do not deform G-type AFM matrix. In this G-type structure, there are no FM interactions along any direction, and the presence of these clusters does not induce any additional FM interaction. In fact, it seems that when the FM cluster concentration increases, that is, for $x < 0.93$, they couple in such a way that the cluster size does not grow up but a new C-type AFM order is dealt. In this C-type structure, there are FM interactions along one direction. In this way, C-type structure appears as G-type AFM disappears; that is, the whole material adopts the C-type structure at $x = 0.85$.

It is remarkable that the proposed model predicts the existence of FM clusters, observed by different experimental techniques, but also allows quantifying, in a very simple way, its shape, number, size, and the associated magnetic moment value. Furthermore, the saturation magnetization value of the material can be calculated.

A different situation is found in the $0 < x \leq 0.15$ range. In this case, Ca^{2+} attracts Mn^{4+}, giving rise to FM clusters whose m_s can be calculated, as already done in the $0.85 \leq x < 1$ range. However, this is not possible because a direct ratio between both values does not exist. This can be understood taking into account that $LaMnO_3$ is an A-type AFM matrix, that is, is FM in the *ab* plane while AFM interactions are present along the *c* axis, and, consequently, the above FM clusters easily perturb the matrix, inducing an increase of the cluster size. Indeed, the experimental results show that in this region the FM clusters present 2–4 nm diameters.[9,27,28]

Therefore, the magnetic behavior exhibited by extreme values of $La_{1-x}Ca_xMnO_3$ can be explained according to the same mechanism: Mn^{4+} is located close to Ca^{2+} in the lanthanum-rich region, and Mn^{3+} is located close to La^{3+} in the opposite side. It is, however, noticeable and remains an open question the fact that although both $LaMnO_3$ and $CaMnO_3$ compounds exhibit similar magnitude order resistance values, doping with Ca and La, respectively, gives rise

(27) Algarabel, P. A.; De Teresa, J. M.; Blasco, J.; Ibarra, M. R.; Kapusta, Cz.; Sikora, M.; Zajac, D.; Riedi, P. C.; Ritter, C. *Phys. Rev. B* **2003**, *67*, 1344021–6.

(28) Alonso, J. M.; Arroyo, A.; Cortés-Gil, R.; García, M. A.; González-Calbet, J. M.; González, J. M.; Hernando, A.; Rojo, J. M.; Vallet-Regí, M. *J. Magn. Magn. Mater.* **2005**, *290–291*, 482–485.

to a different repose. Actually, the substitution of 1% La is followed by an abrupt decrease in the $CaMnO_3$ resistance, whereas it is practically not affected for $LaMnO_3$ when 1% Ca is introduced.

Conclusions

A model is proposed, on the basis of the Mn^{3+} location around La^{3+}, which explains qualitatively and quantitatively the origin and size of the FM droplets responsible for CMR. The appearance of nanometric size clusters, either for low or for high x values, that is, for hole and electron doping regions, respectively, in $Ln_{1-x}A_xMnO_3$ systems results as a consequence of the localization effect that the doping cation (Ca^{2+} or La^{3+}) exerts on the new oxidation state of Mn, to keep the lattice electroneutrality. Once the clusters are formed, they are able to alter the matrix in different extension depending on its magnetic ordering. The asymmetry and complexity of the magnetic phase diagrams in $Ln_{1-x}A_xMnO_3$[3,6,7] can be understood on the basis of the different clusters' ability to perturb the surrounding AFM matrix.

Acknowledgment. Financial support from Ministerio de Educación y Ciencia (Spain) for the research project MAT2004-01248 is acknowledged.

CM800240V